AOI: 10.11234.2024.00021
ACT2024: Special Proceedings of Applied Computer Technology

Adaptive Interference Mitigation in Intelligent Transport Systems: Hadamard vs. Allan Variance Approaches

Charu Priya S, Deepa T

Department of Electronics and Communication Engineering
SRM Institute of Science and Technology, Kattankulathur - 603203, INDIA

ABSTRACT

Vehicular Visible Light Communication (VVLC) presents a promising alternative to traditional radio frequency (RF) technologies in Intelligent Transport Systems (ITS) due to its immunity to electromagnetic interference and use of existing light-emitting diode (LED) infrastructure. This study investigates the performance of a Hadamard variance-based adaptive Normalized Least Mean Squares (NLMS) filter for noise cancellation in VVLC systems, comparing it to the previously established Allan variance-based filter. The analysis reveals that while Allan variance excels at low signal-to-noise ratios (SNRs) by efficiently handling white noise, Hadamard variance demonstrates superior performance at high SNRs by mitigating the impact of random walk noise and linear drifts more effectively. This study's results indicate that the Hadamard variance-based adaptive filter improves bit error rate (BER) performance significantly, especially in high SNR conditions, thus enhancing the reliability and efficiency of VVLC systems in varying noise environments.

Keywords: Intelligent Transport System (ITS), Visible Light Communication (VLC), solar interference, Allan variance, Hadamard variance.

I. INTRODUCTION

Intelligent transport systems, commonly known as ITS, combine modern communication technologies and automotive infrastructures. ITS focuses on improving overall road safety by enhancing traffic management, reducing congestion, and avoiding collisions [1]. The most crucial step in ITS is the information exchange between the vehicles and other infrastructures that previously relied on radio frequency (RF) technology. The necessity of alternate and supplementary communication technologies arises from RF's limited bandwidth and electromagnetic interference constraints [2], [3]. Hence, optical wireless communication emerges as a promising solution. Vehicular visible light communication (VVLC) is a subset of VLC, where the existing light-emitting diode (LED) infrastructures, such as headlamps, tail lamps, and daytime running lamps, send data via the visible light. Since these LED components are already available in the vehicles, it is easy to implement VVLC with additional signal processing units. This technology leverages the immunity of visible light to electromagnetic interference to ensure reliable transportation [2].

Despite the mentioned advantages, VVLC has challenges like solar radiation and other ambient or artificial light interference. The interference effect of sunlight in the form of additional shot noise arising from the statistical fluctuation of the number of photons received is a major VVLC performance degradation factor. Other ambient light interferences include visible light from street lights, vehicle headlights, and other neon display board lights [4]. Apart from these interference sources, factors such as temperature changes, aging of components, and vehicular motion introduce a linear drift in frequency. Hence, it is necessary to improve the signal quality for superior performance [5]. Cutting-edge modulation techniques, adaptive power control, and selective combined receiver structure improved signal-to-noise ratio (SNR) [6], [7], [8], [9]. However, the sun's luminance varies with the wavelength, geographical location, time, and other environmental factors [10], [11]. Thus, the adaptive filters can successfully guide the adjustment to fluctuating interference conditions. This flexibility of VVLC systems to adapt to interference variations ultimately leads to an improved SNR. The previous work included Allan variance to adaptively update the parameters of the adaptive filters for higher performance [12]. It effectively mitigated the noise interference-induced autocorrelation.

In this study, Allan variance in the above-mentioned adaptive noise canceller is compared with the performance of Hadamard variance. Both variances measure the noise characteristics and system stability over time. Allan variance, generally used in oscillator stability analysis, is effectively used to analyze time-correlated noise. Meanwhile, Hadamard variance is supported in environments with high-frequency noise fluctuations and linear drifts. Section 2 illustrates the noise analysis of Hadamard variance. The proposed design of a Hadamard variance-based adaptive noise canceller is in Section 4. The comparison outcomes are mentioned in Section 4, and the closure of this article is in Section 5.

II. HADAMARD VARIANCE NOISE ANALYSIS

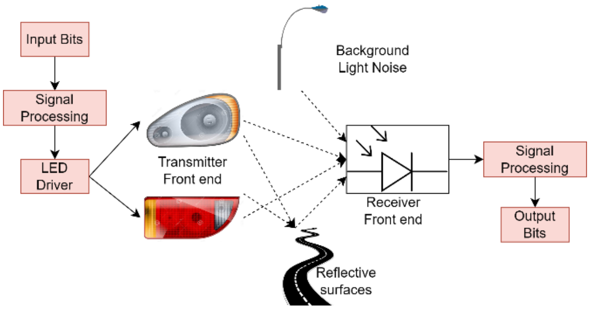

Fig. 1. Vehicular transmission scenario

Hadamard or three-sample variance is another method for analyzing the frequency stability of time-varying data [13]. It is a modified version of Allan variance [14], [15], which uses three consecutive observations instead of two. This makes it robust against linear drifts and long-correlated noises [16]. The vehicular communication scenario in the presence of interferences is given in Fig.1. TR_t is the time-varying input data transmitted by the vehicle headlamp system to the receiver on another vehicle across a non-linear visible light channel. The received data is RX_t, where h_t is the channel model, and V_t is the noise interference.

$$\mathrm{RX_t} = [(\mathrm{TR_t} \otimes \mathrm{h_t}) + \mathrm{V_t}] \tag{1}$$

τ_t is the total cluster time given by $\tau_t = p.t_s$, where 'p' is the number of clusters ($l = 1, 2, \cdots, p$), and t_s is the sampling time. The Hadamard three-sample variance is [13]:

$$\sigma^2_{hvar}(\tau_t) = \frac{1}{6(P_t-p+1)}\left\{\sum_{l=1}^{P_t-p+1}\left[\hat{y}_{l+2p}(p) - \hat{y}_{l+p}(p) + \hat{y}_l(p)\right]^2\right\} \tag{2}$$

P_t is the number of sampling points. Thus, each cluster's Hadamard variance is computed and plotted against the cluster times in a log-log scale. When a noise's power spectral density (PSD) follows the power-law dependence on frequency, it is known as the power-law noise. The Hadamard variance is related to the PSD, $S_y(f)$, as:

$$\sigma^2_{hvar}(\tau_t) = 2^4 \int_0^\infty S_y(f)\frac{\sin^6(\pi f \tau_t)}{(\pi f \tau_t)^2}df \tag{3}$$

The slope of the Hadamard variance (μ) in a log-log plot is related to the spectral index (α) of the power law given by μ=-(α+1)/2. Among the different power-law noise types, the most prevalent noises in a VVLC system are white noise (α=0) and random walk noise (α=-2). Factors like ambient light sources, multipath reflections, and thermal noise in electronic components give rise to white noise. In contrast, slow variations in sunlight intensity, vehicular motion, vibration, and temperature fluctuations lead to linear frequency drifts and long-term correlated random walk noise. Fig.2 shows the variance plot of noises computed using both Allan variance and Hadamard variance.

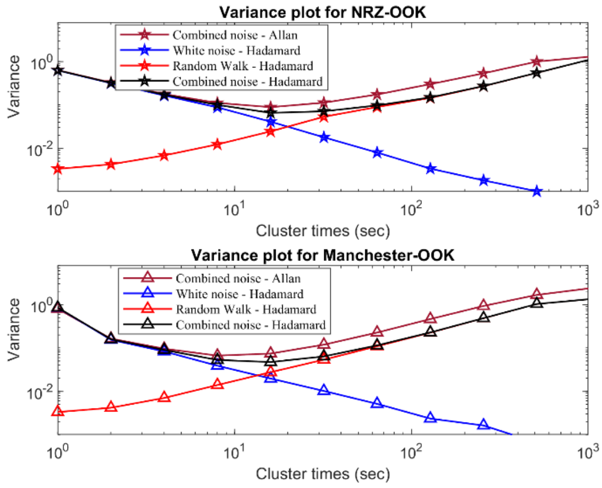

Fig. 2. Allan and Hadamard Variance plot for noise signals

The variance of white noise remains the same for both variances since white noise mainly consists of random fluctuations [17]. Allan variance is the measure of the difference between the consecutive averages [14], [15]. Hence, it is sensitive to low-frequency noises and overestimates them. However, Hadamard variance measures the second difference between the three successive samples and is less sensitive to low-frequency noise and linear drifts. This second difference operation acts as a high-pass filter (α<0), reducing the impact of long-term correlated noises.

III. PROPOSED HADAMARD VARIANCE-BASED ROBUST INTERFERENCE MITIGATOR

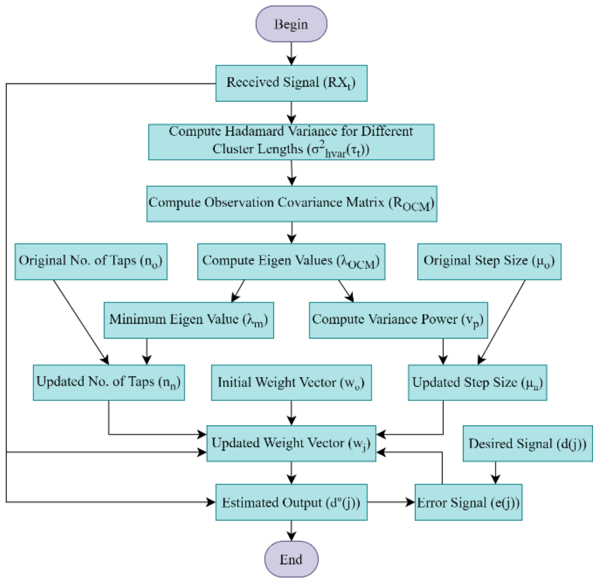

Fig. 3. Flowchart of proposed NLMS interference mitigator

The adaptive filter is a suitable signal-processing method for mitigating interference. The VVLC system's non-stationary behavior is constantly updated through the filter coefficients, so they can dynamically update their response to the changing non-linear conditions. The normalized least mean squares (NLMS) is a straightforward stochastic gradient descent robust noise elimination procedure that minimizes the mean squared error (MSE) between the useful signal and the error signal. The simplified flowchart of the proposed Hadamard variance-based NLMS interference mitigator is given in Fig.3. The observation variance matrix (R_{OCM}) is computed by Hadamard variance values obtained for each cluster. It is a diagonal matrix that signifies the noise is uncorrelated between each distinct cluster.

$$R_{OCM} = diag\left[\sigma^2_{hvar}(\tau_1), \sigma^2_{hvar}(\tau_2), \dots, \sigma^2_{hvar}(\tau_p)\right] \quad (4)$$

The Eigenvalue of this diagonal matrix is nothing but the Hadamard variance values of each cluster. A larger Eigenvalue depicts a more significant variance value, showing that the particular cluster contributes more to noise.

$$\lambda_{OCM}(l) = \sigma^2_{hvar}(\tau_l) \quad (5)$$

The NLMS's step size determines the weights' update rate. It decides how fast the filter coefficients are adjusted in response to the error signal. It affects the convergence rate and stability. The updated step size (μ_n) is given by:

$$\mu_n = \frac{\mu_o}{\beta + v_p} \quad (6)$$

where μ_o is the initial step size of each iteration, β is a constant small positive value to avoid division by zero, and v_p is the total variance power given by:

$$v_p = \sum_{l=1}^{p} \lambda_{OCM}(l) \quad (7)$$

The number of taps determines the length of the NLMS filter, the filter's complexity, and convergence speed. The updated number of taps (n_n) is computed from the original number of taps (n_o) and minimum Eigenvalue (λ_m) as:

$$n_n = n_o + (n_o * \lambda_m) \quad (8)$$

Thus, the NLMS adaptive filter is given by:

$$d^{\circ}(j) = RX_j^T w_{j-1} \quad (9)$$

$$e(j) = d(j) - d^{\circ}(j) \quad (10)$$

$$w_j = w_{j-1} + \frac{\mu_n \,.\, RX_j^* \,.\, e(j)}{\|RX_j\|^2 + \epsilon} \quad (11)$$

$d^{\circ}(j)$ is the estimated output from the NLMS filter. $e(j)$ is the error difference between the desired signal and the estimated output. w_j is the weight vector, determining the filter coefficients at iteration j. This coefficient vector's updation is done so that the MSE is minimal. $\|RX_j\|^2$ is the normalization factor, which comprises the energy of the input signal to enhance stability. ϵ is the small positive constant to avoid dividing by zero.

IV. RESULTS AND DISCUSSION

The data to be transmitted is encoded by non-return-to-zero (NRZ) or Manchester encoding with on-off keying (OOK) modulation. OOK is a case of amplitude shift keying (ASK) with two amplitude levels (0 and 1) [18], [19]. OOK is a smooth, low-complex modulation method usually suggested for vehicular communication systems. The modulation and demodulation equations are [19]:

$$TR_t = tr_t \,.\, [A_t * cos(2\pi f_c\, t)] \quad (12)$$

$$RX_t^{\circ} = \begin{cases} 1, if\ d^{\circ}(t) \geq T_t \\ 0, if\ d^{\circ}(t) < T_t \end{cases} \quad (13)$$

where A_t is the magnitude of the visible light signal, f_c is the carrier frequency and T_t is the demodulation threshold. Within the context of this manuscript, the proposed Hadamard variance-based robust interference mitigator is compared with the previous work of Allan variance-based adaptive noise canceller. The initial step size (μ_o) is 0.032, the original number of taps (n_o) is 32, and the initial weight vector is 0. Fig.4 depicts the variance plot for the system with the proposed filter design at SNRs of 10 dB and 20 dB. White noise has a similar effect on Allan and Hadamard variances since it is a random fluctuation in the signal. In the case of three sample-Hadamard variance, it can filter out the impact of random walk noise and is more specialized in handling linear drifts. Hence, it smoothens out these long-term correlations better than Allan variance.

Understanding the nature of noise types is necessary before analyzing the system's performance. White noise affects the signal with a constant PSD at all frequencies. White noise contribution is dominant at low SNR conditions, particularly when the desired signal is weaker than the noise power. However, though it produces the same effect at high SNR, the desired high-power signal can mask the effect of white noise. When it comes to random walk noise, the interference at any point accumulates the previous values over time. This long-term correlation can introduce significant deviations even at high SNR since the signal cannot mask this accumulated effect.

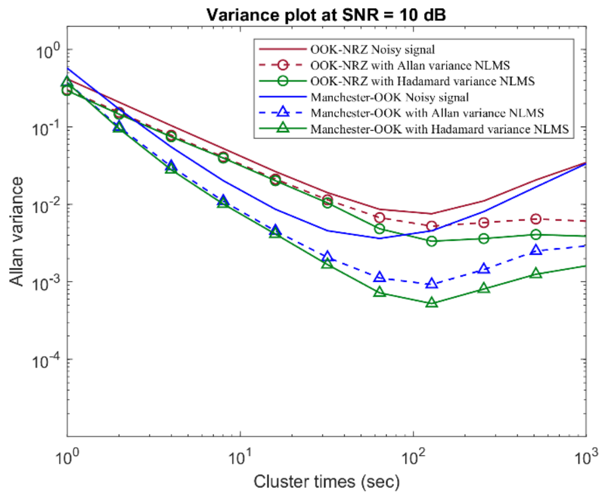

Fig. 4. Variances of proposed Hadamard variance-based robust interference mitigator at 10 dB of SNR.

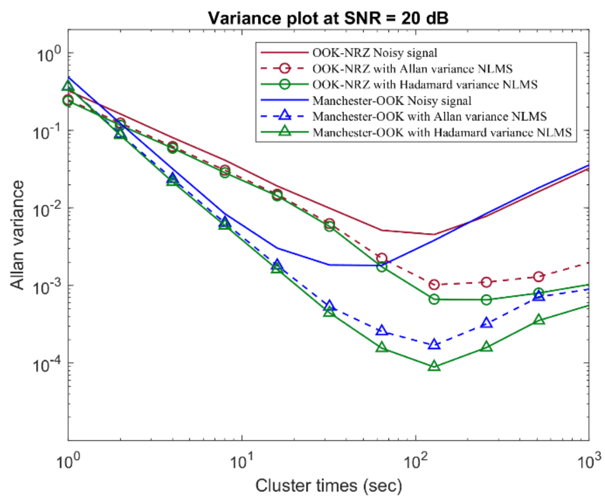

Fig. 5. Variances of proposed Hadamard variance-based robust interference mitigator at 20 dB of SNR.

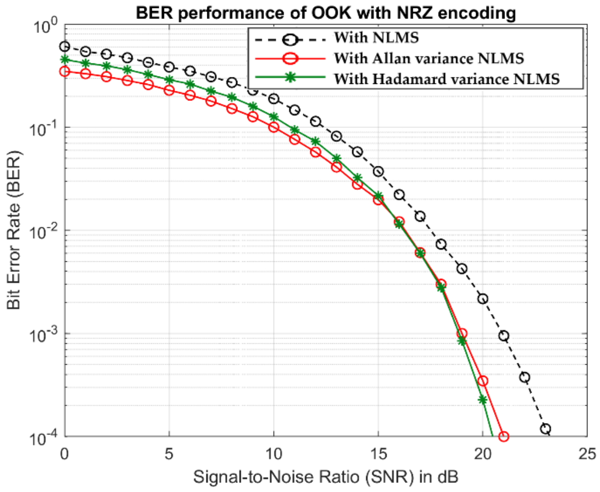

Fig. 6. SNR vs. BER of the system with proposed interference mitigator with NRZ encoding

TABLE I
SNR VS. BER OF THE SYSTEM WITH PROPOSED INTERFERENCE MITIGATOR

Interference mitigator	5 dB SNR	10 dB SNR	20 dB SNR
NRZ Encoded – Allan Variance NLMS	0.22839	0.10023	0.00034
NRZ Encoded - Hadamard Variance NLMS	0.28920	0.12641	0.00022
Manchester Encoded – Allan Variance NLMS	0.20765	0.07372	0.00033
Manchester Encoded – Hadamard Variance NLMS	0.26620	0.09391	0.00015

The SNR vs. BER performance of the vehicular communication system with the proposed mitigator is shown in Fig.5 and Table 1. At low SNR (say 10 dB), Allan variance performs better than Hadamard variance by 21% for both encoding types. This is because the effect of white noise is similar for both variances, but owing to the trade-off of the additional computational burden of the second difference, where Allan variance can perform the work more efficiently. At high SNR (say 20 dB), Hadamard variance is better since it can filter out the random walk interference and linear drifts more efficiently than Allan variance. Here, the BER performance of Hadamard variance is 35% higher than Allan variance for NRZ encoding and 55% for Manchester encoding. Also, the Manchester signal is less influenced by its former state succeeding a conversion, and owing to its balanced distribution; the auto-correlation decreases rapidly.

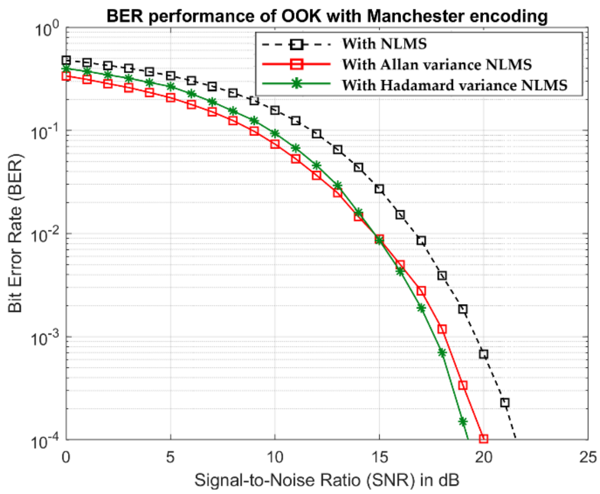

Fig. 7. SNR vs. BER of the system with proposed interference mitigator with Manchester encoding

IV. CONCLUSION

From the above results, this study reveals that the Hadamard variance is more effective than the Allan variance in a VVLC system, particularly in high SNR conditions, due to its superior handling of random walk noise and linear drifts. The Allan variance-based adaptive NLMS filter is sufficient in low SNR scenarios. Its unique ability to update its filter coefficients to maintain a minimum mean squared error is a crucial feature of a reliable and robust VVLC system. This adaptability ensures high-quality data transmission, even in significant ambient disturbances. Looking ahead, future work will focus on extending this promising design to other higher modulation methods, catering to applications that require higher data rates, such as infotainment or multimedia.

REFERENCES

[1] N. H. Hussein, C. T. Yaw, S. P. Koh, S. K. Tiong, and K. H. Chong, "A Comprehensive Survey on Vehicular Networking: Communications, Applications, Challenges, and Upcoming Research Directions," 2022, *Institute of Electrical and Electronics Engineers Inc.* doi: 10.1109/ACCESS.2022.3198656.

[2] L. Cheng, Y. Wu, C. Xu, K. Ashraf, and A. Ashok, "Automotive Visible-Light Communication: Alternative Devices and Systems," *Tsinghua Sci Technol*, vol. 28, no. 4, pp. 719–728, 2023.

[3] M. S. M. Gismalla *et al.*, "Survey on Device to Device (D2D) Communication for 5GB/6G Networks: Concept, Applications, Challenges, and Future Directions," *IEEE Access*, vol. 10, pp. 30792–30821, 2022, doi: 10.1109/ACCESS.2022.3160215.

[4] M. Ahmed, M. A. Atta, J. Farmer, Z. Dawy, D. O'Brien, and A. Bermak, "Multidomain Suppression of Ambient Light in Visible Light Communication Transceivers," *IEEE Transactions on Intelligent Transportation Systems*, vol. 23, no. 10, pp. 18145–18154, Oct. 2022, doi: 10.1109/TITS.2022.3162635.

[5] N. A. Alhaj *et al.*, "Integration of Hybrid Networks, AI, Ultra Massive-MIMO, THz Frequency, and FBMC Modulation Toward 6G Requirements: A Review," *IEEE Access*, vol. 12, pp. 483–513, 2024, doi: 10.1109/ACCESS.2023.3345453.

[6] SHAO-WEI WANG *et al.*, "A high performance blue filter for a white led based visible light communication system," *IEEE Wirel Commun*, vol. 22, no. 2, pp. 61–67, 2015, [Online]. Available: 10.1109/MWC.2015.7096286

[7] Hasan Farahneh, Sikder M. Kamruzzaman, and Xavier Fernando, "Differential Receiver as a Denoising Scheme to Improve the Performance of V2V-VLC Systems," in *2018 IEEE International Conference on Communications Workshops (ICC Workshops)*, 2018, pp. 1–6. [Online]. Available: 10.1109/ICCW.2018.8403726

[8] T. Deepa and H. Mathur, "Performance Analysis of Digitized Orthogonal Frequency Division Multiplexing System for Future Wireless Communication," *Wirel Pers Commun*, vol. 109, no. 4, pp. 2239–2250, Dec. 2019, doi: 10.1007/s11277-019-06678-3.

[9] S. Charu Priya and T. Deepa, "CEMD Solar Noise Suppression for OFDM based Visible Light Vehicular Communication," in *2023 2nd International Conference on Electrical, Electronics, Information and Communication Technologies, ICEEICT 2023*, Institute of Electrical and Electronics Engineers Inc., 2023. doi: 10.1109/ICEEICT56924.2023.10157347.

[10] M. S. Islim *et al.*, "The Impact of Solar Irradiance on Visible Light Communications," *Journal of Lightwave Technology*, vol. 36, no. 12, pp. 2376–2386, Jun. 2018, doi: 10.1109/JLT.2018.2813396.

[11] Mohamed Sufyan Islim and Harald Haas, "An investigation of the solar irradiance effect on visible light communications," in *2017 IEEE 28th Annual International Symposium on Personal, Indoor, and Mobile Radio Communications (PIMRC)*, 2017, pp. 1–6.

[12] S. Charu Priya and T. Deepa, "Design and analysis of allan variance based adaptive noise canceller for vehicular visible light communication," *Opt Quantum Electron*, vol. 56, no. 5, p. 792, Mar. 2024, doi: 10.1007/s11082-024-06679-y.

[13] Capt Steven T. Hutseil, "Relating the Hadamard Variance to MCS Kalman Filter Clock Estimation," in *27th Annual Precise Time and Time Interval (PTTI) Applications and Planning Meeting*, 1996.

[14] D. W. Allan and J. Levine, "A Historical Perspective on the Development of the Allan Variances and Their Strengths and Weaknesses," *IEEE Trans Ultrason Ferroelectr Freq Control*, vol. 63, no. 4, pp. 513–519, Apr. 2016, doi: 10.1109/TUFFC.2016.2524687.

[15] L. Hua, Y. Zhuang, L. Qi, J. Yang, and L. Shi, "Noise Analysis and Modeling in Visible Light Communication Using Allan Variance," *IEEE Access*, vol. 6, pp. 74320–74327, 2018, doi: 10.1109/ACCESS.2018.2883737.

[16] N. Ashby and B. Patla, "Simulations of the Hadamard Variance: Probability Distributions and Confidence Intervals," *IEEE Trans Ultrason Ferroelectr Freq Control*, vol. 63, no. 4, pp. 636–645, 2016.

[17] T. Walter and W. W. Hansen, "A MULTI-VARIANCE ANALYSIS IN THE TIME DOMAIN," 1993.

[18] G. Amouzad Mahdiraji and E. Zahedi, "Comparison of Selected Digital Modulation Schemes (OOK, PPM and DPIM) for Wireless Optical Communications," 2006.

[19] Y. Kim *et al.*, "Analysis of noncoherent ASK modulation-based RF-interconnect for memory interface," *IEEE J Emerg Sel Top Circuits Syst*, vol. 2, no. 2, pp. 200–209, 2012, doi: 10.1109/JETCAS.2012.2193511.